Thermochimica Acta, 239 (1994) 137–145
Elsevier Science B.V., Amsterdam
SSDI 0040-6031(93)01655-M

Thermoanalytic resolution of hydrogen-influenced reductive events in the decomposition course of ammonium paratungstate

Nasr E. Fouad, Ahmed K.H. Nohman and Mohamed I. Zaki *
Chemistry Department, Faculty of Science, Minia University, El-Minia 61519, Egypt

(Received 21 July 1993; accepted 29 November 1993)

Abstract

Hydrogen-influenced reductive events in the decomposition course of ammonium paratungstate (APT) were resolved by thermal analysis (TG and DTA) as a function of the heating atmosphere (air, N_2 and H_2) and rate (2–20°C min^{-1}). A kinetic characterization of the events was carried out non-isothermally. The results indicated that the reductive events begin after the complete decomposition of APT into WO_3 near 400°C, and lead eventually to the formation of W^0 at 700–800°C. Thus, it was concluded that a pre-calcination of APT-containing materials might develop upon reduction to monolayer-type W^0 catalysts.

INTRODUCTION

WO_x species (with $x = 3–0$) constitute the active phase in catalysts for metathesis [1], hydrotreating [2], hydrogenolysis [2] and selective reduction [3, 4] processes. These species are often precursored by ammonium paratungstate [4, 5], $(NH_4)_{10}(H_2W_{12}O_{42}) \cdot 7H_2O$. Recently, however, WO_3 particles have been used as a precursor for the synthesis of WO_x/Al_2O_3 catalysts, adopting the so-called solid/solid wetting technique [6]. For most applications, the catalyst is formulated in a reductive step by heating in an atmosphere of hydrogen [2–4]. The molecular stoichiometry of the WO_x species thus established is varied depending on the temperature regime applied.

In earlier studies performed in this laboratory, the thermal decomposition course of the paratungstate compound in air has been explored physicochemically [7], and kinetic and thermodynamic parameters of the thermal events encountered have been determined [8]. The paratungstate has been shown [7] to decompose completely into crystalline WO_3 near 400°C, encompassing the formation of intermediate metatungstate $[(NH_4)_5(H_2W_{12}O_{40}) \cdot 7H_2O]$ near 200°C and the collapse of the polytungstate lattice into an amorphous substance at 240–290°C. The WO_3 thus produced has shown [9] a marked

* Corresponding author.

thermal stability on further heating to 1000°C in air. In an atmosphere of hydrogen, however, WO_3 was reduced completely to W^0 near 800°C, via the formation of $WO_{2.72}$ (at 520°C) and WO_2 (at 600°C) as intermediate products [9]. Kinetically, the initial stage of the reduction has been found [9] to be dominated by the formation of WO_2, and to be influenced by strong autocatalytic effects associated with the commencement of formation of W^0. Accordingly, a consecutive autocatalytic model [10] was implemented, whereby dissociative adsorption of H_2 [11] on freshly generated W^0 surfaces has been considered the rate-determining step [9].

The present paper reports and discusses the results of a thermoanalytic study of the influence of the atmosphere (air, N_2 and H_2) on the thermal decomposition course of ammonium paratungstate up to 1000°C. The study, which was designed essentially with the intention of resolving the thermal and reductive events of the decomposition course in H_2, involved a kinetic analysis of the thermoanalytical data as a function of heating rate in order to determine if it is advisable to calcine parent materials of WO_x-based catalysts prior to the H_2-reduction step. Such a pretreatment has been found essential in the preparation of analogous catalyst systems [12].

EXPERIMENTAL

Materials and thermoanalytical techniques

Ammonium paratungstate (denoted APT), $(NH_4)_{10}(H_2W_{12}O_{42}) \cdot 7H_2O$, was a 99% pure product of Fluka AG (Switzerland). It was supplied in a finely divided form, and used as supplied. Crystalline WO_3 was obtained by calcination of APT at 400°C for 5 h, according to Mansour et al. [7]. N_2 and H_2 gases were provided by the Egyptian Company of Industrial Gases (Cairo, Egypt) with a nominal purity of 99%. They were subjected to the appropriate deoxygenating and drying procedures prior to application, as described previously [9].

Thermogravimetry (TG) and differential thermal analysis (DTA) curves were recorded on heating up to 1000°C at various rates ($\beta = 2$–20°C min^{-1}) in a dynamic atmosphere (30 ml min^{-1}), using a model 30H Shimadzu thermal analyzer (Japan). Small portions (20–40 mg) of test samples were used in the TG experiments, and a highly sintered α-Al_2O_3 was the thermally inert reference for the DTA measurements.

Kinetic analysis of thermoanalytical data in hydrogen

To calculate the activation energy ΔE (kJ mol^{-1}) and the frequency factor A (min^{-1}), Kissinger's equation [13] was used

$$\ln(\beta/T^2) = -(\Delta E/R)/T + \ln(AR/\Delta E)$$

It was represented graphically by plotting $\ln(\beta/T^2)$ versus $1/T$, where β is the heating rate and T is the temperature at which the weight-variant (TG) and weight-invariant (DTA) events are maximized. The slope and intercept of the linear relationships obtained (see below) facilitated the calculation of ΔE and A, respectively.

Having been determined, the frequency factor A was used to calculate the activation entropy ΔS (J mol^{-1} K^{-1}), employing the equation [14]

$$\Delta S = R \ln(Ah/kT)$$

where k is Boltzmann's constant, h is Planck's constant and R is the universal gas constant (8.314 J mol^{-1} K^{-1}).

RESULTS AND DISCUSSION

The decomposition course

Figure 1 shows TG curves recorded on heating APT at 2°C min^{-1} in air, N_2 and H_2 atmospheres. Corresponding DTA curves, which were also obtained at 2°C min^{-1}, are shown in Fig. 2. The curves indicate a number of thermal events (denoted I–VIII); only one of them (V) is weight-invariant. The curves also show that events I–V occur irrespective of the atmosphere applied, whereas events VI–VIII only occur in H_2 atmosphere. Thermal characteristics of the events encountered are summarized in Table 1 which includes the physicochemical characteristics of the events as previously identified [7, 9].

Table 1 indicates that irrespective of the nature of the atmosphere, events I–IV lead to the formation of WO_3. It remains thermally stable on further heating up to 1000°C in air or N_2. However, in H_2, WO_3 is reduced on

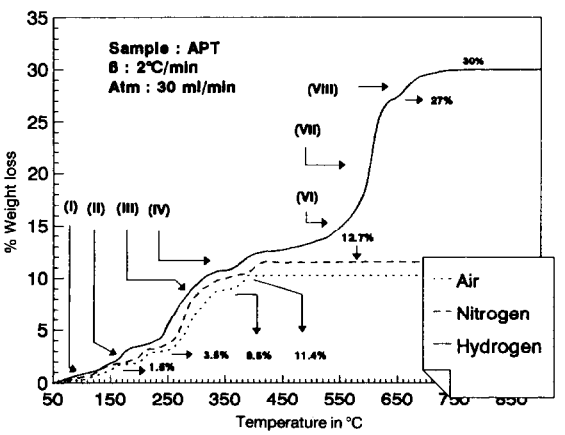

Fig. 1. TG curves recorded on heating APT at 2°C min^{-1} in air, N_2 and H_2.

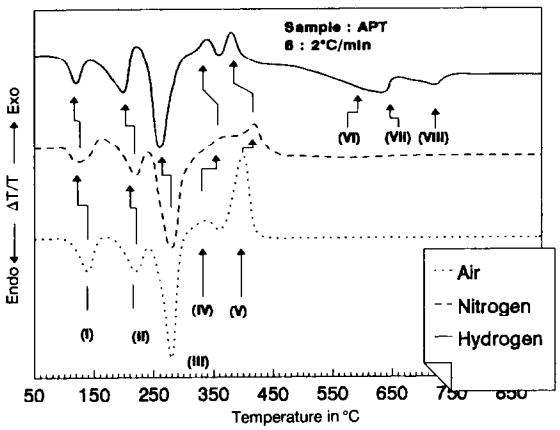

Fig. 2. DTA curves recorded on heating APT at 2°C min^{-1} in air, N_2 and H_2.

TABLE 1

Thermal and physicochemical characteristics of events encountered throughout the decomposition course of APT at 2°C min^{-1} in air (A), nitrogen (N) and hydrogen (H) atmospheres

Event	θ [a]/°C				W.L. [b]	Physicochemical characteristics [c]
	A	N	H		(%)	
I	140	123	100	Endo	1.5	Elimination of CO_3^{2-} and HCO_3^- surface impurities
II	220	215	175	Endo	3.5	Elimination of $(NH_4)_2O$ and transformation into metatungstate
III	280	275	243	Endo	9.5	Loss of hydration water and collapse of polytungstate lattice
IV	330	335	320	Exo	12.0	Formation of WO_3
V	405	415	370	Exo	Invariant	Crystallization of WO_3
VI	–	–	485	Endo	13.7	$WO_3 \rightarrow WO_{2.72}$ ($=W_4O_{11}$)
VII	–	–	600	Endo	20.5	$WO_{2.72} \rightarrow WO_2$
VIII	–	–	660	Endo	30.0	$WO_2 \rightarrow W^0$

[a] Temperatures at which the events are maximized. [b] Cumulative weight loss. [c] Events I–V were characterized in ref. 7, events VI–VIII in ref. 9.

heating at 2°C min^{-1} to $WO_{2.72}$ ($=W_4O_{11}$) at 450–550°C (event VI), WO_2 at 550–610°C (event VII), and eventually to metallic W^0 at 630–690°C (VIII) (Fig. 1). The reductive character of events VI–VIII can be further realized from the comparison, illustrated in Fig. 3, between TG curves obtained on heating APT and bulk WO_3 at 10°C min^{-1} in H_2 atmosphere. The TG curve of WO_3 reveals that the complete reduction into W^0 ($WL_{obs} = 21\%$; $WL_{exp} = 20.7\%$) is achieved near 800°C, and involves three reductive steps corresponding well to events VI–VIII of APT. The results in Fig. 3 confirm that the reducible species in the decomposition products of APT is WO_3.

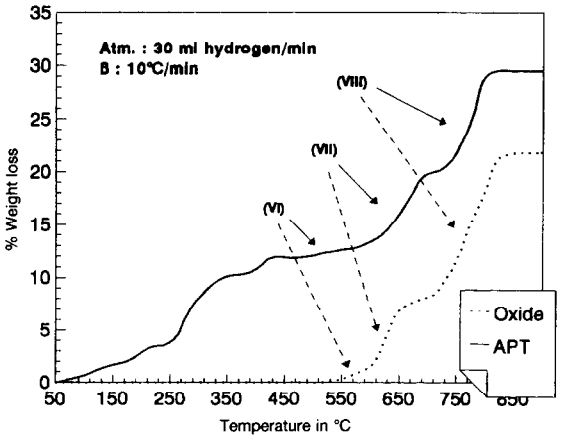

Fig. 3. TG curves recorded on heating APT and WO_3 at 10°C min^{-1} in H_2.

Influence of the heating atmosphere at 2°C min^{-1}

The thermoanalytical curves exhibited in Figs. 1 and 2, and the results summarized in Table 1, elucidate the influence of the surrounding atmosphere on the events encountered during APT decomposition; as follows.

(i) The endothermal events (I–III) accompanying the decomposition of APT into ammonium metatungstate and the subsequent dehydration and collapse of the polytungstate lattice are slightly enhanced upon changing the atmosphere from air to N_2, and subsequently to H_2.

(ii) The exothermic events monitoring the formation (IV) and subsequent crystallization (V) of WO_3 are slightly retarded, but markedly weakened, on replacing air by N_2. In H_2, however, they are partially restored and slightly accelerated.

(iii) The endothermic events VI–VIII only occur in the H_2 atmosphere. They are associated with the reduction steps of WO_3 into W^0.

The paratungstate ion in APT, $(H_2W_{12}O_{42})^{10-}$, consists of corner-sharing groups of three edge-sharing WO_3 octahedra [15]. Each ion is connected to ten others via NH_4^+ ions. The transformation of APT, $(NH_4)_{10}(H_2W_{12}O_{42}) \cdot 7H_2O$, into the metatungstate, $(NH_4)_5(H_2W_{12}O_{40}) \cdot 7H_2O$, is accompanied by the release of $(NH_4)_2O$ species into the gas phase [7]. Thus, the transformation involves deoxygenation. Such a process would be enhanced in a reducing atmosphere. The same applies to the collapse of the polytungstate and formation of WO_3, because it is essentially a polymerization process occurring subsequently to the release of oxygen [7]. In contrast, the exothermic crystallization process of WO_3 (event V) is enhanced in an oxidizing atmosphere. It is retrogressed in H_2, but increased in N_2 atmosphere (Fig. 2).

Despite these effects of different atmospheres, two phenomena remain unchanged: (i) the decomposition events (I–IV) of APT to the onset of

formation of WO_3 occur irrespective of the nature of the surrounding atmosphere; and (ii) events VI–VIII involving the WO_3 thus formed only occur in H_2 atmosphere. Thus, events I–IV are purely heat-induced, whereas events VI–VIII involve a strong chemical influence via H_2 reduction. Accordingly, the former set of events (I–IV) will be described below as being thermal, whereas the latter set (VI–VIII) will be described as being reductive. These two sets of events are well-resolved on the temperature scale at 2°C min^{-1} (Figs. 1 and 2).

Influence of the heating rate in H_2 atmosphere

Figures 4 and 5 show the respective changes in the TG and DTA curves obtained on heating APT with different heating rates (2–20°C min^{-1}) in H_2.

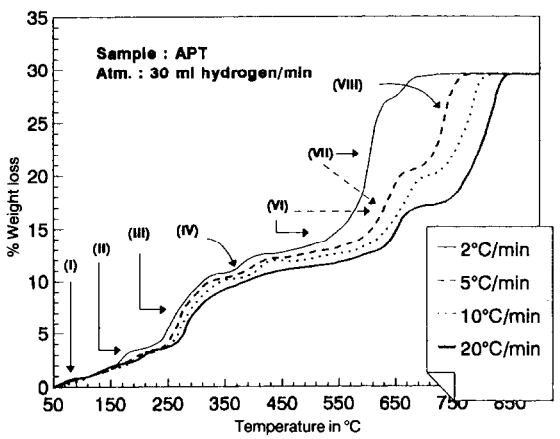

Fig. 4. TG curves recorded on heating APT in H_2 at different heating rates.

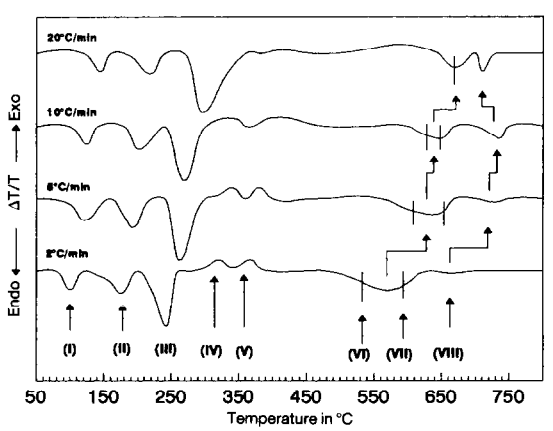

Fig. 5. DTA curves recorded on heating APT in H_2 at different heating rates.

It can be observed that increasing the heating rate results in: shifts to higher temperatures of all the events observed, except for event VIII at 20°C min^{-1}; a weakening of event V; a strengthening of event VIII; and an increasing overlap of events VI–VIII.

Thus, the thermal events I–IV, i.e. APT decomposition to the onset of formation of WO_3, show only a high-temperature shift with increasing heating rate. Such behavior is expected [16], and does not often result in an overlap of events. In contrast, the chemical events VI–VIII, which pertain to the stepwise H_2-reduction of WO_3 into W^0, advance progressively with heating rate towards an almost complete overlap. Figures 4 and 5 show clearly that events VI and VII, which initially overlap at 2°C min^{-1}, appear to merge into a single event at 20°C min^{-1}. These figures also show that the temperature resolution between the now composite VI/VII event and event VIII is minimal at 20°C min^{-1}. This is a result of the sudden low-temperature shift (reversed direction) of event VIII at 20°C min^{-1} (Fig. 5). This unexpected development is evidently associated with the autocatalytic effects characterized previously [9]. The nucleation of W^0 activates a dissociative adsorption of H_2 molecules, which results in a marked promotion of the reduction kinetics [9]. It has been found [9] that the kinetic promotion influences not only the final $WO_2 \rightarrow W^0$ step (event VIII), but also the preceding steps, i.e. $WO_3 \rightarrow WO_{2.72}$ (event VI) and $WO_{2.72} \rightarrow WO_2$ (event VII). These autocatalytic steps also account for the changes in the reductive events VI–VIII as a function of heating rate.

Non-isothermal kinetic parameters

The effects of the heating rate on the temperatures T at which events I–VIII are maximized in H_2, are manifested in Fig. 6 which shows the

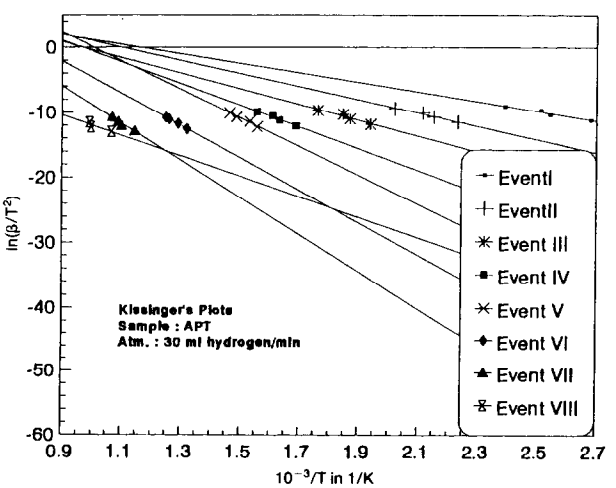

Fig. 6. Kissinger plots for events I–VIII in H_2.

TABLE 2

Non-isothermal kinetic parameters of the thermal (I–V) and reductive (VI–VIII) events occurring during heating of APT in H_2 atmosphere

Event	ΔE/kJ mol^{-1}	ln(A/min^{-1})	r [a]	ΔS/J mol^{-1} K^{-1}
I	61.5	10.6	0.979	−160.1
II	84.4	13.5	0.984	−137.1
III	101.2	14.3	0.976	−131.7
IV	135.9	19.0	0.990	−93.6
V	184.3	25.3	0.985	−41.4
VI	208.2	23.6	0.891	−65.9
VII	238.3	23.0	0.975	−63.1
VIII	131.7	6.5	0.998	−201.9

[a] Correlation coefficient.

Kissinger plots [13]. The kinetic parameters, ΔE and A, derived from these curves and the activation entropy ΔS are given in Table 2, which also includes the correlation coefficient r, so as to monitor the linearity of Kissinger plots (Fig. 6).

Table 2 shows that ΔE increases with the increase in T of each of the events (Table 1), except for event VIII. Thus, the rate-determining step(s) involved becomes more difficult on going from event I to event VII. The contrary behavior of event VIII is probably associated with the autocatalysis operating during this particular event. However, the variation in ΔS reveals that the rate-determining step(s) involved in events I–V increasingly involves a disordering mechanism. Because of the physicochemical characteristics of these events (Table 1), the APT decomposition reactions involved should confirm this disordering which also seems to involve event V in the wake of the retrogressive impacts of H_2 on the crystallization process (Fig. 2). In contrast, the ΔS variation reveals that an ordering mechanism dominates in the reductive events VI–VIII, i.e. formation of W^0. This might be considered to confirm the autocatalytic influence, associated essentially with event VIII ($WO_2 \rightarrow W^0$), on the kinetics of the overall reduction course of the WO_3. These results indicate that the thermal (I–IV) and reductive (VI–VIII) events are resolved, not only thermally but also kinetically.

CONCLUSIONS

The following conclusions can be drawn from the above presented and discussed results.

(i) Heating APT in hydrogen atmosphere establishes a thermal decomposition course to the formation of WO_3 near 400° and a subsequent reduction course of the oxide to metallic W^0. The reduction is completed somewhere between 680 and 800°C, depending on the heating rate.

(ii) The reductive effects of H_2 do not influence the thermal decomposition course of APT at $\leq 400°C$, except for insignificant shifts in the operational temperature regions of the events involved. The reductive effects commence following the formation of WO_3.

(iii) The thermal decomposition (I–IV) and H_2 reduction (VI–VIII) courses are well resolved both thermally and kinetically.

(iv) The reductive synthesis of APT-precursored catalysts should be preceded by a calcination step at 400°C. The WO_3 thus formulated may exchange strong dispersive interactions with the support surface (alumina), which lead, upon reduction, to monolayer-type W^0/Al_2O_3 catalysts [6].

REFERENCES

1 B.C. Gates, Catalytic Chemistry, John Wiley, New York, 1992, p. 311, 342.
2 Z. Paal and P.G. Menon (Eds.), Hydrogen Effects in Catalysis: Fundamentals and Practical Applications, Chemical Industries Series, Marcel Dekker Inc., New York, 1988.
3 H. Bosch and F. Janssen, Catal. Today, 2 (1988) 369.
4 J.P. Chen and R.T. Yang, Appl. Catal., 80A (1992) 135.
5 A. Iannibello, S. Marengo, P. Tittarelli, G. Morelli and A. Zecchina, J. Chem. Soc. Faraday Trans. 1, 80 (1984) 2209.
6 J. Leyrer, R. Margraf, E. Taglauer and H. Knözinger, Surf. Sci., 201 (1988) 603.
7 S.A.A. Mansour, M.A. Mohamed and M.I. Zaki, Thermochim. Acta, 129 (1988) 187.
8 M.A. Mohamed, S.A.A. Mansour and M.I. Zaki, Thermochim. Acta, 138 (1989) 309.
9 N.E. Fouad, K.M.E. Attyia and M.I. Zaki, Powder Technol., 74 (1993) 31.
10 J. Sloczynski, React. Solids, 7 (1989) 83.
11 G.C. Bond and P.A. Sermon, Catal. Rev., 8 (1973) 211.
12 M.I. Zaki, B. Vielhaber and H. Knözinger, J. Phys. Chem., 90 (1986) 3176.
13 H.E. Kissinger, J. Anal. Chem., 29 (1959) 1702.
14 Z. Lu and L. Yang, Thermochim. Acta, 188 (1991) 135.
15 R. Allmann, Acta Crystallogr. Sect. B, 27 (1971) 1393.
16 J. Šesták, V. Satava and W.W. Wendlandt, Thermochim. Acta, 7 (1973) 333.